JACS
JOURNAL OF THE AMERICAN CHEMICAL SOCIETY

Subscriber access provided by American Chemical Society

Article

Theoretical and Experimental Investigations on the Chemical Reactions of Positively Charged Phenyl Radicals with Cytosine and 1-Methylcytosine

Yiqun Huang, and Hilkka Kenttmaa

J. Am. Chem. Soc., **2003**, 125 (32), 9878-9889• DOI: 10.1021/ja021263r • Publication Date (Web): 18 July 2003

Downloaded from http://pubs.acs.org on March 29, 2009

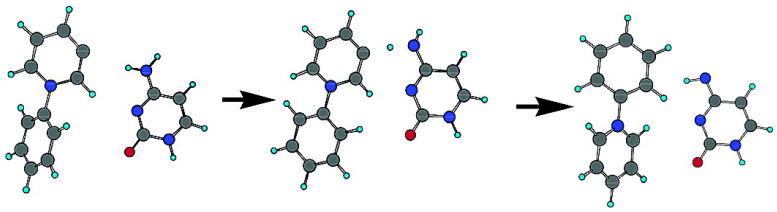

More About This Article

Additional resources and features associated with this article are available within the HTML version:

- Supporting Information
- Access to high resolution figures
- Links to articles and content related to this article
- Copyright permission to reproduce figures and/or text from this article

View the Full Text HTML

ACS Publications
High quality. High impact.

Journal of the American Chemical Society is published by the American Chemical Society. 1155 Sixteenth Street N.W., Washington, DC 20036

J|A|C|S
ARTICLES
Published on Web 07/18/2003

Theoretical and Experimental Investigations on the Chemical Reactions of Positively Charged Phenyl Radicals with Cytosine and 1-Methylcytosine

Yiqun Huang and Hilkka Kenttämaa*

Contribution from the Department of Chemistry, Purdue University, West Lafayette, Indiana 47907-1393

Received October 8, 2002; E-mail: hilkka@purdue.edu

Abstract: The chemical behavior of positively charged phenyl radicals toward cytosine, 1-methylcytosine, and some pyrimidine analogues in the gas phase was investigated both theoretically by performing molecular orbital calculations and experimentally by using FT/ICR mass spectrometry. The phenyl radicals react with cytosine and 1-methylcytosine predominately by hydrogen abstraction and addition. For cytosine, the preferred site for hydrogen abstraction appears to be the amino group, and addition occurs preferentially at the N3 and N1 positions of the keto and enol tautomeric forms, respectively. For 1-methylcytosine, the methyl group is the thermodynamically favored site for hydrogen abstraction and N3 for addition. Possible structures and formation mechanisms are suggested for two unknown product ions formed upon the reaction of cytosine with the 3-dehydro-*N*-phenylpyridinium radical cation.

Introduction

Radical attack on DNA is one of the main reasons for DNA damage.[1,2] For instance, it has been found that aromatic σ,σ-biradicals play an important role in the action of some antitumor drugs, such as the enediyne type antitumor antibiotics. The key step in DNA cleavage by such radicals is hydrogen atom abstraction from the sugar moiety in DNA.[1,2] Therefore, knowledge on the factors that determine the efficiency of the hydrogen abstraction is of importance in the design of antitumor drugs whose function is based on nonhydrolytic cleavage of DNA. Besides aromatic σ,σ-biradicals, many monoradicals formed upon metabolic conversion of organic compounds can also attack a DNA chain by hydrogen abstraction and also by addition to a nucleobase. For instance, electron paramagnetic resonance (EPR) spectroscopy in conjunction with spin-trapping carried out in aqueous solution showed that OH and alkoxyl radicals can attack the C5−C6 double bond (the numbering schemes of pyrimidine bases is given in the discussion section) of the pyrimidine base moiety via addition or the sugar moiety via hydrogen abstraction in nucleosides, nucleotides, and DNA.[3−5] It was also reported that the thiyl radical can attack the C6-position of a pyrimidine nucleoside.[6] Furthermore, benzoyl peroxide can be metabolized to phenyl radicals that can damage DNA.[7]

However, the chemical behavior of phenyl radicals toward DNA and its components has not been extensively investigated.[8] The reactivity of the 4-methoxyphenyl radical (which is believed to behave in the same manner as phenyl radical[8]) toward nucleic acids and their components has been studied in aqueous solution by using EPR spectroscopy coupled with spin trapping.[8] Addition of the radical to a pyrimidine ring and hydrogen abstraction from a sugar moiety were reported. The preferred site for nucleophilic addition in bases appears to be C6. However, under neutral pH conditions, the 4-methoxyphenyl radical was found to add to the C5 position of uracil. Both C5- and C6-adducts were reported for thymine and the latter predominates. No adduct was observed for cytosine at pH 7.4. Under acidic conditions, C6-adducts were reported to be preferred for uracil, thymine, and cytosine.[8] Protonation of the pyrimidine-based nucleobases under acidic conditions was thought to make the pyrimidine ring (especially the electron-deficient C6) more susceptible toward attack by the slightly nucleophilic phenyl radicals.

To eliminate interferences caused by the presence of solvent and to explore the intrinsic chemical reactivity of phenyl radicals toward nucleobases, gas-phase reactions of phenyl radicals with the nucleobases uracil, adenine, and thymine, and some of their derivatives, were investigated in our laboratory by using FT-ICR mass spectrometry.[9] Positively charged, chemically inert groups were introduced into the phenyl radical to form so-called distonic ions[10] via which the phenyl radicals can be manipulated in the mass spectrometer. For uracil and adenine, both addition

(1) Stubbe, J.; Kozarich, J. W. *Chem. Rev.* **1987**, *87*, 1107−1136.
(2) Steenken, S. *Chem. Rev.* **1989**, *89*, 503−520.
(3) Catterall, H.; Davies, M. J.; Gilbert, B. C.; Polack, N. P. *J. Chem. Soc., Perkin Trans. 2* **1993**, 2039−2047.
(4) Davies, M. J.; Gilbert, B. C.; Hazlewood, C.; Polack, N. P. *J. Chem. Soc., Perkin Trans. 2* **1995**, 13−21.
(5) Hazlewood, C.; Davies, M. J. *J. Chem. Soc., Perkin Trans. 2* **1995**, 895−901.
(6) Carter, K. N.; Taverner, T.; Schiesser, C. H.; Greenberg, M. M. *J. Org. Chem.* **2000**, *65*, 8375−8378.
(7) Greenley, T. L.; Davies, M. J. *Biochim. Biophy. Acta* **1993**, *1157*, 23−31.
(8) Hazlewood, C.; Davies, M. J.; Gilbert, B. C.; Packer, J. E. *J. Chem. Soc., Perkin Trans. 2* **1995**, 2167−2174.
(9) Ramirez-Arizmendi, L. E.; Heidbrink, J. L.; Guler, L. P.; Kenttämaa, H. I. *J. Am. Chem. Soc.* **2003**, *25*, 2272−2281.
(10) Yates, B. F.; Bouma, W. J.; Radom, L. *J. Am. Chem. Soc.* **1984**, *106*, 5805−5808.

10.1021/ja021263r CCC: $25.00 **© 2003 American Chemical Society**

and hydrogen abstraction reactions were observed, and the former is favored. In the case of thymine, hydrogen abstraction products were found to be predominant while addition followed by immediate loss of CH_3 was also reported. The observation of the latter reaction indicates that the addition can occur at C5 of thymine.[9] The purpose of the present work is to explore the reactions of a series of substituted phenyl radicals toward cytosine in the gas phase.

Experimental Section

The experiments were carried out by using a Finnigan FTMS 2001 Fourier transform ion cyclotron resonance mass spectrometer (FT/ICR). The instrument contains a differentially pumped dual cell in a magnetic field produced by a 3.0 T superconducting magnet. The nominal base pressure was $<10^{-9}$ Torr, as maintained by two Edwards diffusion pumps (800 L/s), each backed with an Alcatel 2012 mechanical pump. The two cells of the instrument are separated by a metal wall called the conductance limit with a 2 mm hole in the center. All trapping plates were maintained at +2 V unless otherwise specified.

Samples were introduced into the instrument by using Varian leak valves, heated solids probes, pulsed valves, or batch inlet systems equipped with a variable leak valve. The nominal reagent pressures were measured with two ionization gauges, one located on each side of the dual cell.

The reagents used include cytosine, 1,3,5-^{15}N-2,4-^{13}C-cytosine, 1-methylcytosine, 5-methylcytosine hydrochloride, 2-hydroxypyrimidine hydrochloride, 4-aminopyrimidine, and pyrimidine. The positively charged phenyl radicals used in the present work are 3-dehydro-*N*-phenylpyridinium (**a**) and its partially deuterated analogue 3-dehydro-*N*-(D_5-phenyl)pyridinium; *N*-(3-dehydro-5-chlorophenyl)pyridinium (**b**), *N*-(3-dehydrophenyl)pyridinium (**c**), and *N*-(4-dehydrophenyl)pyridinium (**d**). The chemicals used for the generation of these charged phenyl radicals were chlorobenzene, bromobenzene, iodobenzene, D_5-iodobenzene, 3-iodopyridine (KARL industries Inc.), pyridine (Mallinckrodt Specialty Chemicals), 1,3-diiodobenzene, 1,4-diiodobenzene, and 1,3-dichloro-5-iodobenzene. Except for 3-iodopyridine and pyridine, all chemicals were purchased from Sigma-Aldrich. All these chemicals were used without further purification. Charged phenyl radicals were generated using a procedure reported earlier.[11] For the preparation of radical **a**, chlorobenzene (or bromobenzene or iodobenzene) was introduced at a nominal pressure of 6.0×10^{-8} -1.1×10^{-7} Torr into one side of the dual cell by using a batch inlet system. 3-Iodopyridine was introduced at the same nominal pressure into the same cell through a Varian leak valve. For the generation of radicals **b**−**d**, the halobenzene precursors (1, 3-dichloro-5-iodobenzene for radical **b**, 1,3-diiodobenzene for radical **c**, and 1,4-diiodobenzene for radical **d**) were introduced through a Varian leak valve while pyridine was introduced into the same cell through a batch inlet at the same nominal pressure. The mixture was subjected to electron ionization that resulted in the formation of halobenzene radical cations. Typical electron ionization conditions were 20 eV electron energy, 5 μA emission current, and 50 ms ionization time. The halobenzene radical cations were allowed to react with pyridine (for radicals **b**, **c**, and **d**) or 3- iodopyridine (for radical **a**) for 4−5 s. *Ipso*-substitution of a halogen atom yielded abundant substituted halobenzene ions.

The substituted halobenzene ions, generated in one side of the dual cell, were transferred into the other side by grounding the conductance limit plate for about 175−180 μs, which allowed the ions to pass through a 2 mm hole in the center of the plate. The transferred ions were allowed to cool for about 1 s by IR emission and by collisions with the neutral molecules present in this cell. The substituted halobenzene ions were isolated by applying a stored−waveform inverse Fourier transform[12] (SWIFT) excitation pulse to the cell. After isolation, the ions were subjected to homolytic carbon−halogen bond cleavage to form the desired charged phenyl radicals **a**−**d** by using sustained off-resonance irradiated collision-induced dissociation (SORI-CID).[13] SORI-CID was implemented by introducing argon into the cell via a pulsed valve assembly (the nominal peak pressure in the cell was about 1×10^{-5} Torr) and collisionally activating the ions with argon for 0.5−1 s at a frequency 1 kHz higher than the cyclotron frequency of the ions. The charged phenyl radicals were cooled by providing about 400 ms time delay for IR emission, and for collisions with the neutral molecules present in the cell. Charged phenyl radicals were isolated by applying a SWIFT excitation pulse to the cell. The isolated charged phenyl radicals were allowed to react with a reagent for a variable period of time (typically 10−160 s). The reagents were introduced via a heated solids probe (cytosine, 1-methylcytosine, 5-methylcytosine hydrochloride, 4-aminopyrimidine, and 2-hydroxypyrimidine hydrochloride) or batch inlet system (pyrimidine). Detection was performed by using "chirp" excitation of 124 V_{p-p} amplitude, 2.7-MHz bandwidth, and 3.2 kHz/μs sweep rate. All the spectra are the average of 15 transients, which were recorded as 64k data points and subjected to one zero fill prior to Fourier transformation. Each reaction spectrum was background corrected by using a procedure described previously.[14]

Primary product ions were identified on the basis of their fixed relative abundances (branching ratios) at short reaction times. By assuming pseudo-first-order kinetics, the second-order rate constant of each reaction (k_{exp}) was obtained from a semilogarithmic plot of the relative abundance of the reactant ion versus time. A parametrized trajectory theory[15] was employed to calculate the collision rate constants (k_{coll}). The reaction efficiencies are given as k_{exp}/k_{coll}. The accuracy of the rate constant measurements is estimated to be 50% while the precision is better than 10%. The greatest uncertainty arises from the pressure measurement in the cell. The pressure readings of the ion gauges (located remote from the cell) were corrected for the sensitivity of the ion gauges toward each neutral reagent[16,17] and for the pressure gradient between the cell and the ion gauge. The latter correction factor was obtained for each neutral reagent by measuring rates of exothermic electron and proton-transfer reactions assumed to occur at collision rate. In the present work, protonated acetone was utilized as the proton donor while carbon disulfide radical cation was used as the electron acceptor.

The Gaussian 98 program[18] was employed to perform molecular orbital calculations based on density functional theory (DFT). The enthalpy changes (exothermicities) for the hydrogen abstraction from cytosine and 1-methylcytosine by radicals **a**−**d**, the addition of cytosine with radical **c**, and the addition of 1-methylcytosine with radical **a** at absolute zero Kelvin were determined directly by optimizing the geometries of the reactants and products and calculating their corresponding electronic energies at the B3LYP/6-31G(d) level of theory. All optimized geometries were verified to be real local minima by performing frequency analysis (no imaginary frequencies). The corresponding zero point vibrational energies (ZPVE) were calculated at

(11) Heidbrink, J. L.; Thoen, K. K.; Kenttämaa H. I. *J. Org. Chem*. **2000**, *65*, 645−651.

(12) Chen, L.; Wang, T.-C. L.; Ricca, T. L.; Marshall, A. G. *Anal. Chem*. **1987**, *59*, 449−454.

(13) Gauthier, J. W.; Trautman, T. R.; Jacobson, D. B. *Anal. Chim. Acta* **1991**, *246*, 211−225.

(14) Leeck, D. T.; Stirk, K. M.; Zeller, L. C.; Kiminkinen, L. K. M.; Castro, L. M.; Vainiotalo, P.; Kenttämaa, H. I. *J. Am. Chem. Soc*. **1994**, *116*, 3028−3038.

(15) Su, T.; Chesnavich, W. J. *J. Chem. Phys.* **1982**, *76*, 5183−5185.

(16) Miller, K. J.; Savchik, J. A. *J. Am. Chem. Soc*. **1979**, *101*, 7206−7213.

(17) Bartmess, J. E.; Georgiadis, R. M. *Vacuum* **1983**, *33*, 149−153.

(18) Frisch, M. J.; Trucks, G. W.; Schlegel, H. B.; Scuseria, G. E.; Robb, M. A.; Cheeseman, J. R.; Zakrzewski, V. G.; Montgomery, Jr., J. A.; Stratmann, R. E.; Burant, J. C.; Dapprich, S.; Millam, J. M.; Daniels, A. D.; Kudin, K. N.; Strain, M. C.; Farkas, O.; Tomasi, J.; Barone, V.; Cossi, M.; Cammi, R.; Mennucci, B.; Pomelli, C.; Adamo, C.; Clifford, S.; Ochterski, J.; Petersson, G. A.; Ayala, P. Y.; Cui, Q.; Morokuma, K.; Malick, D. K.; Rabuck, A. D.; Raghavachari, K.; Foresman, J. B.; Cioslowski, J.; Ortiz, J. V.; Baboul, A. G.; Stefanov, B. B.; Liu, G.; Liashenko, A.; Piskorz, P.; Komaromi, I.; Gomperts, R.; Martin, R. L.; Fox, D. J.; Keith, T.; Al-Laham, M. A.; Peng, C. Y.; Nanayakkara, A.; Gonzalez, C.; Challacombe, M.; Gill, P. M. W.; Johnson, B.; Chen, W.; Wong, M. W.; Andres, J. L.; Gonzalez, C.; Head-Gordon, M.; Replogle, E. S.; and Pople, J. A., Gaussian, Inc., Pittsburgh, PA, 1998.

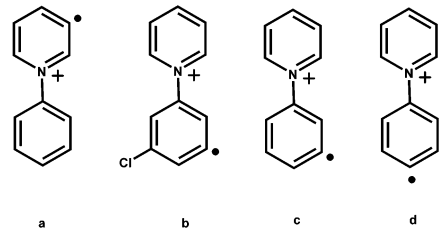

Figure 1. Structures of radicals **a**−**d**.

the same level of theory and used to correct the electronic energy. The zero point energy was scaled by multiplying with a scaling factor of 0.9804.[19] In addition, for the hydrogen abstraction from cytosine by radicals **a**−**d**, the enthalpy changes at 298 K were calculated at the B3LYP/6-31G(d) level of theory by using isodesmic reactions. The 298 K bond dissociation energies (BDE) relevant for hydrogen abstraction from cytosine were estimated at both the B3LYP/6-31G(d) and B3LYP/6-311+G(d,p)//B3LYP/6-31G(d) levels of theory by using isodesmic reactions. The thermal vibrational energy (including zero point energy) was not scaled for 298 K enthalpy change and BDE calculations.

The geometries and energies of transition states for the hydrogen abstraction from cytosine by radicals **a**−**d**, and for the addition of cytosine and radical **c**, were determined by performing transition state calculations at the B3LYP/6-31G(d)+ZPVE level of theory. The transition states were verified as true first-order saddle points along the correct reaction coordinate by frequency analysis (one imaginary frequency corresponding to the vibration along the reaction coordinate which leads to the decomposition of transition state into products).

The enthalpy changes, together with the geometries and energies of the transition states for the adduct formation of protonated cytosine with neutral phenyl radical in acidic aqueous solution, were also estimated at the B3LYP/6-31G(d) level of theory in an effort to explain the different addition behavior of cytosine toward phenyl radicals observed in gas-phase FT-ICR and aqueous EPR experiments. In all aqueous solution calculations, the Onsager model based on the Self-Consistent Reaction Field (SCRF) principle[19] was utilized. SCRF principle regards the function of the solvent as the presence of an evenly distributed electrostatic potential field that can be described by a uniform dielectric constant ϵ. The solvation energy is caused by dipole−dipole interactions between the solute and solvent. Different models for SCRF calculation use different methods to evaluate the shape of the solute molecule in solution. In the Onsager model, the solute molecule is regarded as occupying a cavity with a fixed radius.[19] The dielectric constant ϵ of water was chosen to be 78.39.[18]

Results and Discussion

Radicals **a**−**d** (Figure 1) have been demonstrated[9,11] earlier to undergo gas-phase reactions characteristic of those of the neutral phenyl radical in solution, such as hydrogen abstraction and addition. Therefore, these radicals can be used to model the chemical behavior of neutral phenyl radicals toward nucleobases. In this work, reactions of radical **a** toward all substrates shown in Figure 2 (except for pyridine) and radicals **b**−**d** toward cytosine, 1-methylcytosine, and 5-methylcytosine (Figure 2) were examined in a Fourier transform ion cyclotron resonance mass spectrometer. Radical **a** was found to be the most reactive, followed by radicals **b**, **c**, and **d**. Both hydrogen abstraction and addition reactions were observed upon interaction of radicals **a**−**d** with cytosine and 1-methylcytosine. The reactions of cytosine and 1-methylcytosine are discussed in section 1 and section 2, respectively. The possible structures and formation mechanisms of two major unknown product ions formed upon the reaction of radical **a** with cytosine are addressed in section 3.

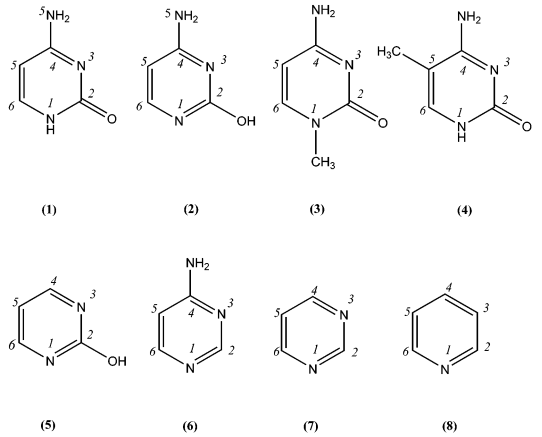

Figure 2. Structures and numbering schemes of keto-cytosine (**1**), enol-cytosine (**2**), 1-methylcytosine (**3**), 5-methylcytosine (**4**), 2-hydroxypyrimidine (**5**), 4-aminopyrimidine (**6**), pyrimidine (**7**), and pyridine (**8**).

Table 1. Overall Reaction Efficiency and Product Branching Ratios[a] Measured for the Reactions of Cytosine wth Radicals **a**−**d**

		product branching ratios (%)				
					unknown ions	
radical	overall efficiency (%)	hydrogen abstraction	adduct	adduct-H	*m*/*z* 172	*m*/*z* 173
a	70	34	6	2	28	30
b	7	63	37	0	0	0
c	3	66	34	0	0	0
d	2	70	30	0	0	0

[a] Overall efficiency and product branching ratios are the averaged values of several repeated experiments.

1. Reactions between Charged Phenyl Radicals and Cytosine. 1.1. Overall Reaction Efficiencies and Branching Ratios of the Products. The major reactions between cytosine and the charged phenyl radicals **a**−**d** are hydrogen abstraction and addition (sometimes followed by the loss of a hydrogen atom to form a closed-shell species). The overall reaction efficiencies ($k_{exp}/k_{coll} \times 100\%$) and product branching ratios are given in Table 1. The total reaction efficiency depends on the structure of the charged phenyl radical, ranging from 70% for **a** to 2% for **d**. The less reactive radicals favor hydrogen abstraction more than addition. The hydrogen abstraction and addition reactions are discussed separately below. In addition, the reactions of radical **a** with cytosine yield two abundant unprecedented product ions of *m*/*z* 172 (28%) and 173 (30%). The possible structures and formation mechanisms of these two product ions are briefly discussed in section 3.

1.2. Hydrogen Abstraction. The two main goals of the present investigation of hydrogen abstraction from cytosine were to determine the preferred sites for hydrogen abstraction and to explore the influence of radical structures on the hydrogen abstraction efficiency. Both kinetic and thermodynamic factors have to be taken into account. The kinetic factors are discussed in the transition state calculations section. The thermodynamic factors include the relative stabilities of the hydrogen abstraction products, the bond dissociation energies of the relevant C−H, O−H, and N−H bonds in the cytosine molecule, and the reaction enthalpy changes (exothermicity). These are discussed below.

(19) Foresman, J. B.; Frisch, Æ. *Exploring Chemistry with Electronic Structure Methods*, 2nd ed.; Gaussian Inc.: Pittsburgh, PA, 1996; Chapter 10.

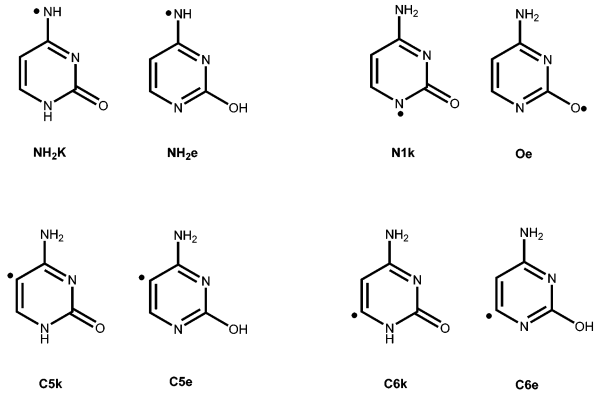

Figure 3. Structures of the products that may be formed upon hydrogen abstraction from cytosine by radicals **a**−**d**.

Table 2. Relative Stabilities of the Different Hydrogen Abstraction Products That May Be Formed upon the Reactions between Cytosine and Radicals **a**−**d** As Calculated at the B3LYP/6-31G(d)+ZPVE Level of Theory

products	electronic *E* (hartree)	ZPVE (hartree)	*E* + 0.9804ZPVE (hartree)	relative stability (kcal/mol)
keto-based				
NH_2k	−394.2575766	0.0847430	−394.1744946	0.00
N1k	−394.2456245	0.0857940	−394.1615121	8.15
C5k	−394.2361292	0.0856390	−394.1521687	14.01
C6k	−394.2432644	0.0847200	−394.1602049	8.97
enol-based				
NH_2e	−394.2616882	0.0850730	−394.1782826	0.00
Oe	−394.2456245	0.0857950	−394.1615111	10.52
C5e	−394.2343663	0.0861910	−394.1498646	17.83
C6e	−394.2467472	0.0860080	−394.1624250	9.95

In the gas phase, the keto and *trans*-enol forms are the two most stable tautomers of cytosine. Both tautomers have nearly equal energies.[20,21] Therefore, in the gas phase, both the keto and *trans*-enol tautomers of cytosine need to be taken into account. Hence, hydrogen abstraction from cytosine by radicals **a**−**d** can yield any or all of eight different isomeric products. These products are shown in Figure 3 and they are referred to as **NH_2k**, **NH_2e**, **N1k**, **Oe**, **C5k**, **C5e**, **C6k**, and **C6e**. Here **k** and **e** stand for the keto and *trans*-enol tautomers, respectively, and **NH_2**, **N1**, **O**, **C5**, and **C6** indicate the hydrogen donor sites.

1.2.1. Relative Stabilities of the Hydrogen Abstraction Products, the Bond Dissociation Energies, the Reaction Enthalpy Changes, and the Thermodynamically Preferred Hydrogen Abstraction Sites in Cytosine. The relative stabilities of eight isomeric cytosine radicals were estimated by a direct comparison of their electronic energies and scaled zero point vibrational energies. The results are listed in Table 2. According to the relative thermodynamic stability, the most favored hydrogen abstraction site is the amino group (more favored than other sites by at least 8 kcal/mol). The calculated low spin densities on the amino nitrogen atom (0.78 for **NH_2k** and 0.70 for **NH_2e**) indicate that the unpaired electron in these structures has some π character and can interact with the π electron system of the cytosine ring, which helps to stabilize the structures **NH_2k** and **NH_2e**. Due to a different orbital symmetry, the unpaired σ electron cannot interact with the π electron system of the cytosine ring for structures **C5k**, **C5e**, **C6k**, and **C6e**. The calculated spin densities at the radical site are 0.94 for **C5k**, 0.96 for **C5e**, 0.89 for **C6k**, and 0.86 for **C6e**. The high spin density at the radical sites of these isomers indicates a relatively localized unpaired σ electron. The lower spin density on C6 of **C6k** and **C6e** than that on C5 of **C5k** and **C5e** structures results from the presence of nitrogen (N1) adjacent to C6 that polarizes the C6−N1 bond,[22] which helps to delocalize the spin density centered on C6 and stabilize the structure. Geometry optimization of the structure **N1k** converged to the structure **Oe** with the spin density highly localized on the carbonyl oxygen (0.96).

The relevant homolytic bond dissociation energies (BDE) of cytosine at 298 K were calculated by using the isodesmic reaction 1 and eq 2:

$$\text{cytosine} + \text{R}^{\cdot} \rightarrow \text{(cytosine-H)}^{\cdot} + \text{RH} \qquad (1)$$

$$\text{BDE(cytosine-H)} = \Delta H_{298} + \text{BDE(RH)} \qquad (2)$$

Here (cytosine-H)$^{\cdot}$ is the cytosine radical formed upon the loss of a hydrogen atom from the cytosine molecule and RH is a reference molecule with a known homolytic 298 K bond dissociation energy. ΔH_{298} is the calculated enthalpy change of reaction 1 at 298 K. Benzene, aniline, and phenol, and the corresponding radicals, were chosen as reference systems. The experimental 298 K BDE data for these reference systems are BDE(H−C_6H_5) = 110.9±2.0 kcal/mol, BDE(H−NHC_6H_5) = 88.0±2 kcal/mol, and BDE(H−OC_6H_5) = 86.5±2 kcal/mol.[23] Also chosen as reference systems were pyrrole (BDE(H−N) = 96.6±4 kcal/mol), pyridine (BDE(H−C3) = 112±2 kcal/mol), and pyrimidine (BDE(H−C6) = 103±2 kcal/mol, BDE(H−C5) = 112±2 kcal/mol).[22] Some of the reference systems were used for isodesmic reaction-based enthalpy change calculations only (discussed below). The numbering schemes for pyrimidine and pyridine are shown in Figure 2.

The isodesmic reactions designed for BDE calculations are shown in Figure 4. The recommended BDE values of cytosine are summarized in Table 3. The BDE values predicted by the B3LYP/6-31G(d) and B3LYP/6-311+G(d,p)//B3LYP/6-31G(d) levels of theory are very similar. The N5−H bond of the amino group is the weakest one, followed by the C6−H bond. The C6−H bond is much weaker than the C5−H bond because of the polarization by the adjacent C6−N1 bond.[22] The C5−H and N1−H bonds (for keto tautomer), as well as the O−H bond (for enol tautomer), are relatively strong. Therefore, BDE calculations predict that hydrogen abstraction from NH_2 is the most energetically favored, followed by abstraction from C6.

The 298 K enthalpy changes for hydrogen abstraction from different sites in cytosine by radicals **a**−**d** estimated by using isodesmic reactions and the 0 K enthalpy changes obtained from direct calculations are shown in Table 4. Both isodesmic reaction-based 298 K enthalpy change calculations and direct 0 K enthalpy change calculations predict that hydrogen abstraction from the NH_2 group is the most exothermic for all radicals. Direct enthalpy calculations also predict that hydrogen abstractions from N1 of keto-cytosine and the hydroxyl group of enol-cytosine are exothermic, but isodesmic reaction-based enthalpy calculations show that these reactions are endothermic except

(20) Leś, A.; Adamowicz, L.; Bartlett, R. J. *J. Phys. Chem.* **1989**, *93*, 4001−4005.
(21) Gould, I. R.; Burton, N. A.; Hall, R. J.; Hillier, I. H. *J. Mol. Sturct. (THEOCHEM)* **1995**, *331*, 147−154.
(22) Barckholtz, C.; Barckholtz, T. A.; Hadad, C. M. *J. Am. Chem. Soc.* **1999**, *121*, 491−500, and references therein.
(23) McMillen, D. F.; Golden, D. M. *Annu. Rev. Phys. Chem.* **1982**, *33*, 493−532.

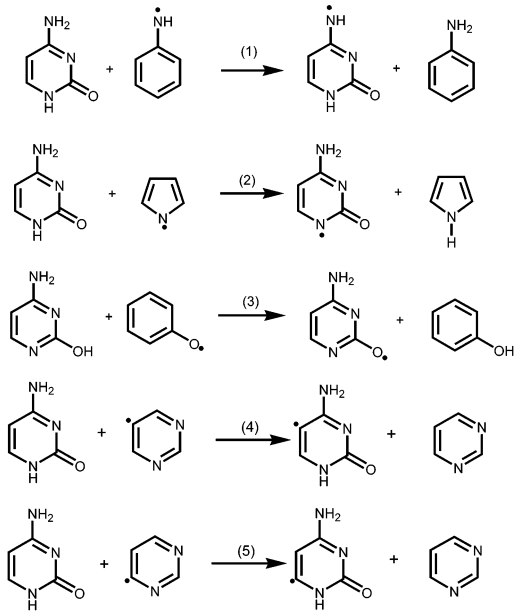

Figure 4. Isodermic reactions used to calculate the BDEs of N5-H (1), N1-H (2), C5-H (4), and C6-H (5) bonds of keto-cytosine and the O-H bond (3) of enol-cytosine. The isodermic reactions similar to (1), (4), and (5) were used to calculate the BDEs of the N5-H, C5-H, and C6-H bonds of enol-cytosine, respectively.

Table 3. Some 298 K Homolytic Bond Dissociation Energies of Cytosine Calculated Using Isodesmic Reactions at the B3LYP/6-31G(d) and B3LYP/6-311+G(d,p)//B3LYP/6-31G(d) Levels of Theory (kcal/mol)

	B3LYP/6-31G(d)	B3LYP/6-311+G(d,p)//B3LYP/6-31G(d)
keto-cytosine		
H−N5	101.8	102.7
H−C5	113.5	113.7
H−C6	107.0	107.7
H−N1	114.5	114.9
enol-cytosine		
H−N5	98.1	98.5
H−C5	113.6	113.5
H−C6	104.2	104.3
H−O	113.7	113.9

for the reactions involving radical **a**. Because of possible computational errors caused by the basis set and correlation effects, the results derived from the isodesmic reaction-based methods are expected to be most reliable.

All four different types of calculations (relative stability, BDE, direct enthalpy change, and isodesmic reaction-based enthalpy change) predict that the most favored hydrogen abstraction site is the amino group. In addition, all four types of calculations predict that the C5 site is not energetically favored for hydrogen abstraction.

1.2.2. Influence of Polar Effects and Transition State Calculations. Hydrogen abstraction from the same site of the same tautomeric form of cytosine by the different radicals **b**−**d** (Table 4) is associated with almost the same enthalpy change (enthalpy change difference is less than 0.16 kcal/mol), but these reactions are less exothermic by about 3 kcal/mol than hydrogen abstraction by radical **a.** The reaction efficiencies for hydrogen abstraction from cytosine by radicals **b**−**d** are 4%, 2%, and 1%, respectively (derived from Table 1). Therefore, some other factors besides enthalpy differences are contributing to the transition state energies of the reaction.

Table 4. Enthalpy Changes[a] of Hydrogen Abstraction from Cytosine by Radicals **a**−**d** Calculated at the B3LYP/6-31G(d) Level of Theory (kcal/mol)

Keto-cytosine Based Hydrogen Abstraction Product

	NH_2k		N1k		C5k		C6k	
radical	isodesmic	direct	isodesmic	direct	isodesmic	direct	isodesmic	direct
a	−14.98	−16.39	−2.26	−8.24	−3.24	−2.38	−9.76	−7.42
b	−11.44	−13.47	1.28	−5.33	0.30	0.54	−6.22	−4.51
c	−11.34	−13.37	1.38	−5.23	0.41	0.64	−6.12	−4.41
d	−11.48	−13.52	1.24	−5.37	0.26	0.49	−6.26	−4.55

Enol-cytosine Based Hydrogen Abstraction Product

	NH_2e		Oe		C5e		C6e	
radical	isodesmic	direct	isodesmic	direct	isodesmic	direct	isodesmic	direct
a	−18.67	−20.08	−3.08	−9.56	−3.18	−2.25	−12.57	−10.13
b	−15.13	−17.16	0.47	−6.64	0.36	0.67	−9.03	−7.21
c	−15.03	−17.06	0.57	−6.54	0.46	0.77	−8.93	−7.11
d	−15.17	−17.21	0.42	−6.68	0.32	0.62	−9.07	−7.26

[a] "Direct" enthalpy changes were calculated directly from the enthalpies of reactants and products at 0 K while "isodesmic" enthalpy changes were calculated by using isodesmic reactions at 298 K.

The transition state (energy barrier) for hydrogen abstraction by radicals is the result of an avoided crossing of the ground state and some excited states along the reaction coordinate.[24−26] The transition state, therefore, can be represented as a resonance hybrid of the ground state and the relevant excited state configurations. On the basis of the nature of the reactants, both covalent and ionic excited states can strongly interact with the ground state.[24−26] If the ionic excited state contributes strongly to the transition state, the transition state is said to be stabilized by polar effects.[24,25] For hydrogen abstraction, a recent ionic avoided curve crossing model[26] can offer a good qualitative description of the origin of the energy barrier. For positively charged phenyl radicals, the most important physical parameter that controls the relative barrier height is the electron affinity of the radical.[27] The larger the electron affinity of the radical, the greater its reactivity. For radicals **a**−**d**, the vertical electron affinities were estimated at the B3LYP/6-31+G(d) level of theory. In the case of radical **a**, the positive charge is located in the same ring as the radical site, which results in low electron density at the radical site and a high electron affinity (vertical EA = 5.78 eV). Radical **a** has the greatest reactivity among the four radicals. The presence of an electron-withdrawing Cl atom in the *meta*-position with respect to the radical site in radical **b** also helps to lower the electron density and hence increase the electron affinity at the radical site (vertical EA = 5.11 eV). Radical **c** has a vertical EA (4.87 eV) that is lower than that of radical **b** because of the absence of electron-withdrawing substituents. Therefore, radical **c** is expected and was observed to be less reactive than radical **b**. The large distance between the positively charged group and the radical site in radical **d** causes the largest electron density at the radical site among the four radicals and, in turn, the smallest electron affinity (vertical EA = 4.5 eV) and the least reactivity.

(24) Pross, A.; Yamataka, H.; Nagase, S. *J. Phys. Org. Chem.* **1991**, *4*, 135−140.
(25) Wong, M. W.; Pross, A.; Radom, L. *J. Am. Chem. Soc*. **1994**, *116*, 6284−6292.
(26) Clarke, J. S.; Kroll, J. H.; Donahue, N. M.; Anderson, J. G. *J. Phys. Chem. A* **1998**, *102*, 9847−9857.
(27) Tichy, S. E.; Thoen, K. K.; Price, J. M.; Ferra, J. J.; Petucci, C. J.; Kenttämaa, H. I. *J. Org. Chem*. **2001**, *66*, 2726−2733.

To determine whether the model discussed above adequately describes hydrogen abstraction from cytosine by radicals **a**−**d**, the transition states were investigated by performing molecular orbital calculations. Transition state calculation is a challenging task in modern quantum chemistry and computational chemistry because the geometry of the transition state cannot be measured directly. The size of our systems restricts the utilization of larger basis sets and high-level post Hartree−Fock methodologies. However, for simple hydrogen abstraction reactions of the type $R_1 + R_2H \rightarrow R_1H + R_2$ (R_1 = H, CH_3, NH_2, and OH radicals, R_2 = H or CH_3), B3LYP/6-31G(d) calculations have been reported to provide good transition state energies.[28] Therefore, this level of theory was utilized in the transition state calculations for hydrogen abstraction from cytosine by radicals **a**−**d**.

The potential energy surface profile of a bimolecular substitution reaction in the gas phase is different from that in solution. In the gas phase, there are no solvent molecules to stabilize reactant molecules. Therefore, the separated reactants in the gas phase usually have a higher energy than in solution. When two reactant molecules approach each other, they can form a reactant-like ion−molecule complex with a lower energy. Along the reaction pathway, the complex will overcome the energy barrier (transition state) to form a product-like complex and ultimately release the products. The Brauman's double-well model [29−31] is often used to describe the potential energy surface of gas-phase ion−molecule reactions. In many cases, the energy barrier is negative with respect to the separated reactants because the reacting system is stabilized by ion/dipole and ion-induced dipole interactions between the reactants. Although the energy barrier is negative, its further lowering can still accelerate the reaction unless the barrier lies substantially lower in energy than the isolated reactants. The geometries of the electrostatically bound ion−molecule complexes are difficult to determine due to the very flat potential energy surface in the vicinity of the complexes. Therefore, the absolute energy difference between the reactant-like complex and transition state cannot be estimated accurately. However, the efficiencies of bimolecular ion−molecule reactions in the gas phase can be estimated by RRKM theory which does not require information on the reactant-like complexes. [29−31]

The lowest energy transition states for hydrogen abstraction from cytosine by radicals **a**, **c**, and **d** are illustrated in Figures 5a−f. The transition state structures involving radical **b** are omitted because they closely resemble the corresponding transition states involving radical **c**. In these figures, the transition states are referred to as **TS(**α, *β***)**, where α refers to one of the radicals **a**, **c**, and **d** and *β* represents the hydrogen abstraction product, such as **NH_2k**, **N1k**, etc. The transition state structures **TS(**α, **NH_2e)** and **TS(**α, **C5e)** are omitted because they are similar to **TS(**α, **NH_2k)** and **TS(**α, **C5k)**, respectively. The transition state energies relative to the total energy of the separated reactants are shown in Table 5. Figure 6 illustrates the calculated double-well type potential energy surface profile of hydrogen abstraction from the keto-cytosine by radical **a** to form the product **NH_2k**.

To explore the correlation between the calculated energy barriers and the measured reaction efficiencies, the energies of different transition states formed upon the interaction of the same cytosine tautomer with the different radicals **a**−**d** for the same reaction pathway (to form the same hydrogen abstraction product) were compared. It can be seen from Table 5 that the transition state related to radical **a** always has the lowest energy, followed by the transition state related to radical **b**. The transition state involving radical **d** has the highest energy. This is consistent with the experimental results (Table 1) and the trends predicted by the ionic avoided curve crossing model (based on electron affinity differences among the radicals **a**−**d**). In all cases, the calculated relative energy of the transition state related to radical **a** is lower than the corresponding transition state related to radical **b** by 1.40−4.52 kcal/mol. This energy difference reflects the large vertical EA difference between radicals **a** and **b** (0.67 eV). On the other hand, the EA difference between radicals **b** and **c** is only 0.24 eV, which explains why the transition state related to radical **b** lies only 0.20−0.78 kcal/mol lower in energy than the corresponding transition state involving radical **c**.

Table 5. Energy Barriers (Relative to the Energies of the Separated Reactants) of Hydrogen Abstraction from Cytosine by Radicals **a**−**d** Calculated at the B3LYP/6-31G(d)+ZPVE Level of Theory (kcal/mol)

Keto-cytosine Based Hydrogen Abstraction Product

radical	NH_2k	N1k	C5k	C6k
a	−8.14	−9.13	6.09	3.70
b	−6.74	−5.21	8.79	6.66
c	−6.31	−4.64	9.12	6.98
d	−0.42	−1.43	9.37	7.01

Enol-cytosine Based Hydrogen Abstraction Product

radical	NH_2e	Oe	C5e	C6e
a	−7.48	−7.59	3.85	−5.07
b	−2.96	−3.79	6.92	−0.69
c	−2.35	−3.59	7.36	0.09
d	−0.27	−2.71	7.60	0.84

The transition state formed upon the interaction of cytosine with radical **d** is higher in energy than the transition state related to radical **c**. However, the magnitude of the energy difference varies significantly for different reaction pathways. The likely reason for this phenomenon is that, besides the polar effect, the ion−dipole interaction can also play a role in lowering the energy barrier. For instance, for the transition states along the reaction pathways that lead to the formation of the products **NH_2k**, **NH2e**, and **N1k**, the cytosine ring can orient itself with respect to radical **c** in such a way that the most electronegative oxygen atom of cytosine approaches the positively charged site of radical **c** to achieve effective ion−dipole interaction that helps to lower the barrier. Such ion−dipole interaction is not available for radical **d** (Figures 5a,b). Therefore, the relatively large energy barrier differences in these cases are likely caused by both polar effects and ion−dipole interactions. In contrast, an effective ion−dipole interaction cannot be achieved by radical **c** in the transition states leading to the formation of the products **C5k** and **C5e**. Consequently, the cytosine ring prefers a partially vertical orientation with respect to the phenyl ring and the pyridine ring in order to minimize steric hindrance. For the radical **d**, the large distance between the radical and charge sites prevents a stabilizing ion−dipole interaction (Figure 5d). Therefore, polar effects are the main factor causing the energy barrier differences between transition states related to radicals

(28) Skokov, S.; Wheeler, R. A. *Chem. Phys. Lett.* **1997**, *271*, 251−258.
(29) Olmstead, W. N.; Brauman, J. I. *J. Am. Chem. Soc.* **1977**, *99*, 4219−4228.
(30) Asubiojo, O. I.; Brauman, J. I. *J. Am. Chem. Soc.* **1979**, *101*, 3715−3724.
(31) Dodd, J. A.; Brauman, J. I. *J. Phys. Chem.* **1986**, *90*, 3559−3562.

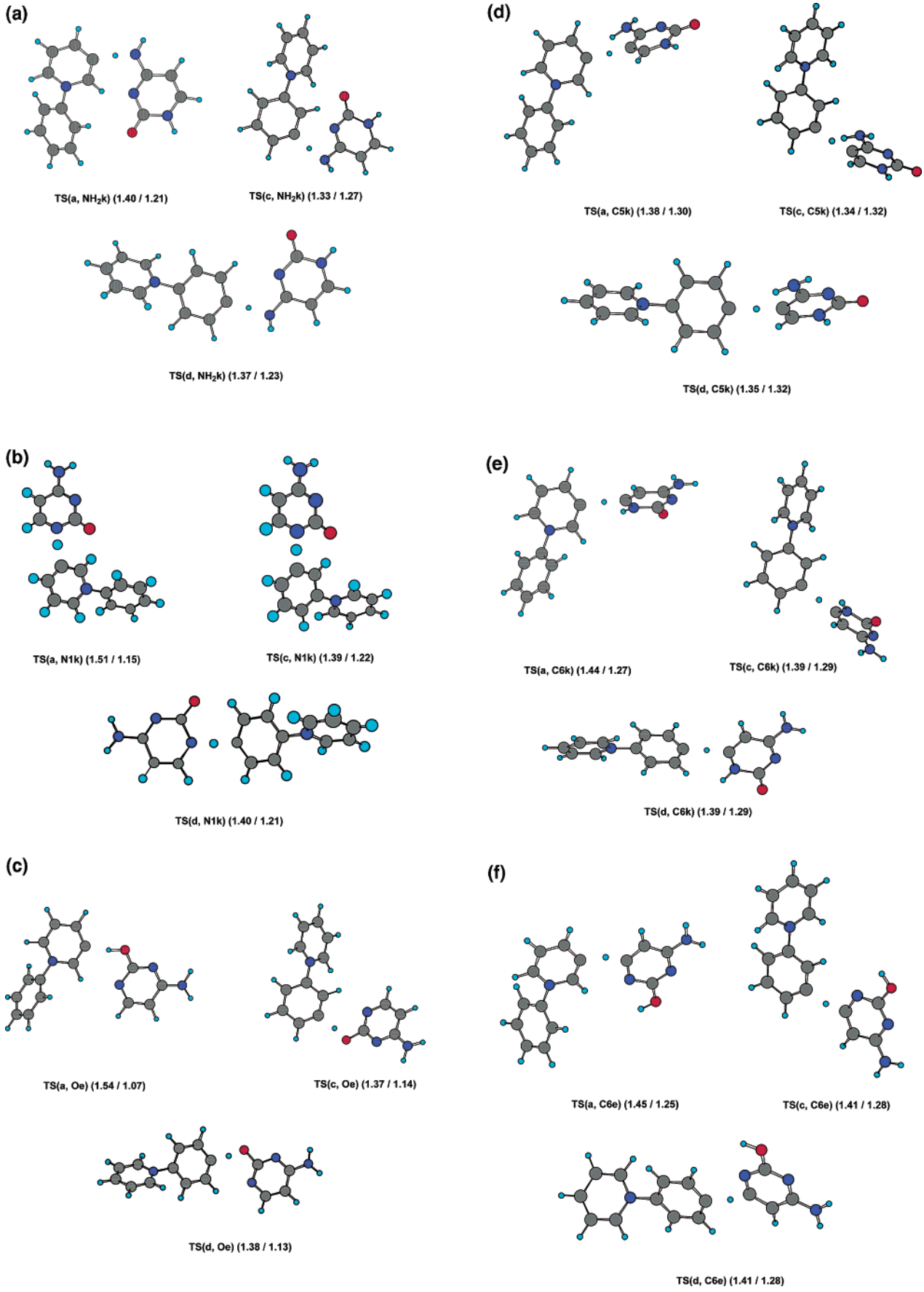

Figure 5. Transition state structures calculated at the B3LYP/6-31G(d)+ZPVE level of theory for hydrogen abstraction from cytosine by radicals **a**, **c**, and **d** to form the products (a) **NH_2k**, (b) **N1K**, (c) **Oe**, (d) **C5k**, (e) **C6k**, and (f) **C6e**. The numbers in parenthesis correspond to the distance between the reaction site of the radical and the hydrogen atom, and the distance between the hydrogen atom and the reaction site of cytosine, respectively, in Å.

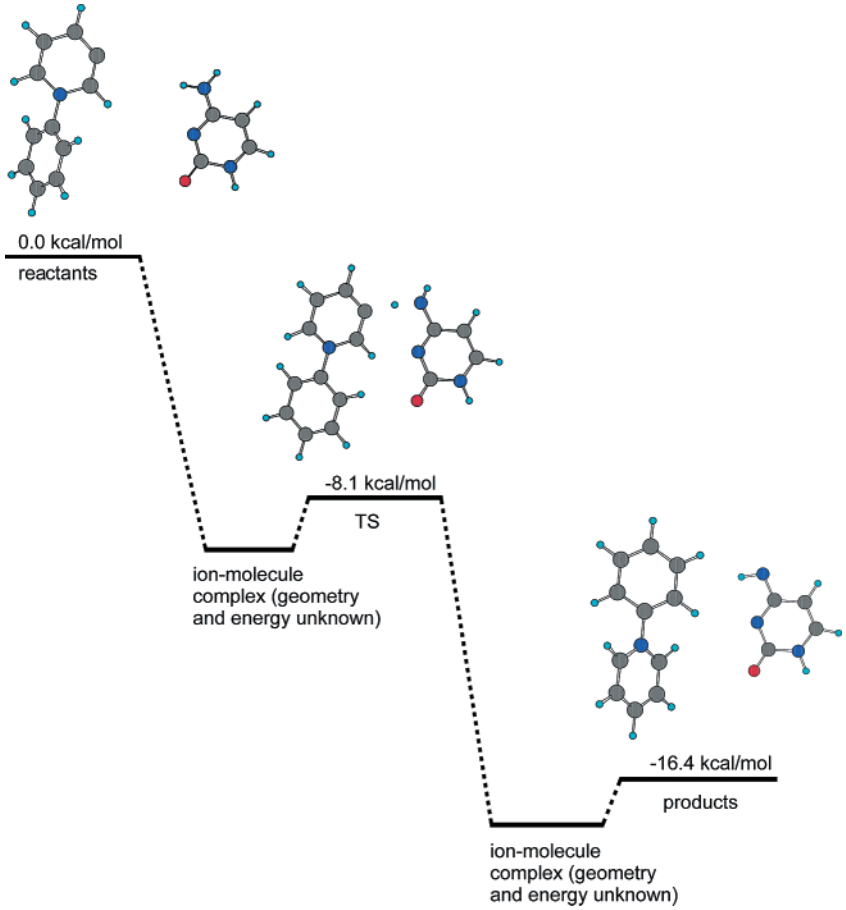

Figure 6. Potential energy surface calculated at the B3LYP/6-31G(d)+ZPVE level of theory for hydrogen abstraction from keto-cytosine by radical **a** to form the product $\mathbf{NH_2k}$.

c and **d**: 0.25 kcal/mol for the **C5k** pathway and 0.24 kcal/mol for the **C5e** pathway. The same situation is true for the **C6k** pathway where the energy difference is only 0.03 kcal/mol (Figure 5e). For **C6e** and **Oe** formation pathways, it is also difficult for the oxygen atom of cytosine to approach the positively charged site of radicals **c** and **d**, and the ion−dipole interactions are weak (Figure 5c and 5f). Therefore, the energy barrier differences mainly result from polar effects due to the 0.37 eV EA difference of radicals **c** and **d**: 0.75 kcal/mol for the **C6e** pathway and 0.88 kcal/mol for the **Oe** pathway, respectively.

On the basis of our transition state calculations, the formation of structures $\mathbf{NH_2k}$ and $\mathbf{NH_2e}$ upon hydrogen abstraction from cytosine by the positively charged phenyl radicals appears to be both thermodynamically most favored (large enthalpy change) and kinetically favored (low energy barrier). Hydrogen abstractions from N1 of keto cytosine and oxygen of enol cyosine also have low energy barriers, but may not be thermodynamically favored.

1.3. Addition and Other Reactions. Another major reaction between cytosine and the positively charged phenyl radicals is addition (sometimes followed by a hydrogen atom loss). Possible structures of adducts of cytosine and radical **c** are shown in Figures 7a and 7b. The structures of adducts of cytosine and radical **a** were also calculated (not shown) and found to be very similar to the adducts shown in Figures 7a and 7b.

It is difficult to examine the addition site experimentally. However, an investigation on the gas-phase reactions of positively charged phenyl radicals **a**−**d** with 5-methylcytosine revealed adducts that did not dissociate by loss of a methyl radical. These results suggest that the addition does not occur at the C5 position since addition to the methylated carbon atom of thymine and its derivatives is followed by a rapid methyl loss.[9]

The enthalpy changes for the formation of adducts shown in Figures 7a and 7b were calculated directly due to the lack of suitable reference systems whose experimental BDE data are available. The optimization of the C2 adduct failed to achieve convergence at the B3LYP/6-31G(d) level of theory. The structure is sterically highly hindered. Therefore, it is reasonable to assume that the likelihood for the formation of the structure is small and the addition of the charged phenyl radicals to C2 is not energetically favored.

According to the calculated addition enthalpy changes, the thermodynamically preferred addition site for the keto-cytosine is N3, followed by the carbonyl oxygen, C5 and C6. For the enol-cytosine, N1 is the energetically favored site, followed by N3, C5, and C6. C4 addition is the least energetically favored for both keto and enol tautomers.

Energy barriers for the formation of adducts shown in Figures 7a and 7b were obtained by transition state calculations at the B3LYP/6-31G(d)+ZPVE level of theory. For the keto-cytosine, addition of radical **c** to N3 has the lowest energy barrier (−8.08 kcal/mol), followed by the addition to O, C5, and C6 (−6.68, −5.39, and −3.82 kcal/mol, respectively). Addition to C4 has the highest energy barrier (8.15 kcal/mol). For the enol-cytosine,

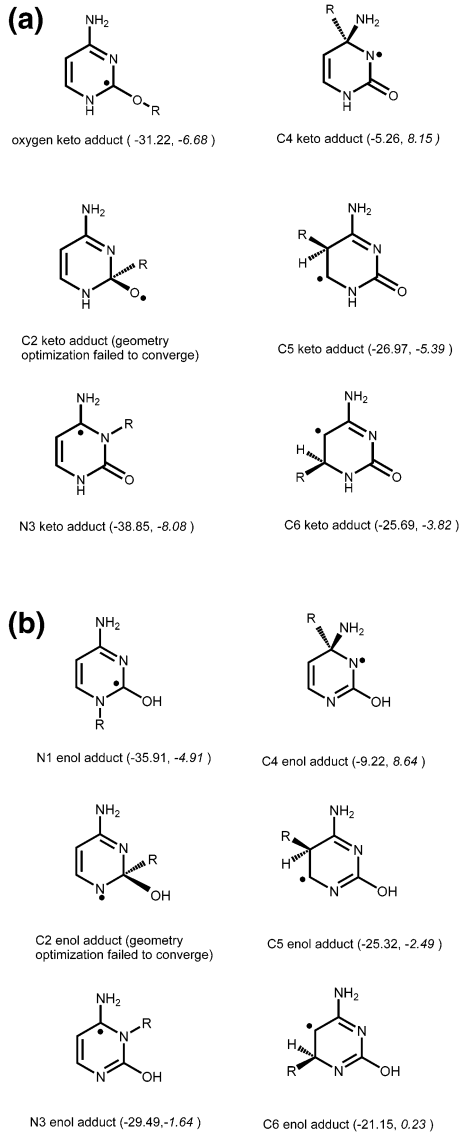

Figure 7. Structures of adducts possibly formed upon the gas-phase reactions of (a) keto-cytosine and (b) enol-cytosine with radical **c** (R). The addition enthalpy changes and energy barriers (in italics) are given in parentheses in kcal/mol.

addition of radical **c** to N1 has the lowest energy barrier (−4.91 kcal/mol), followed by addition to C5, N3, C6, and C4 (−2.49, −1.64, 0.23, and 8.64 kcal/mol, respectively). In most cases, the kinetically preferred addition sites (based on transition state calculations) are consistent with the thermodynamically favored ones. In conclusion, addition of radical **c** in keto and enol cytosine to N3 and N1, respectively, is kinetically as well as thermodynamically preferred. Radicals **a**, **b**, and **d** are assumed to have similar addition site preference toward cytosine.

The charge density distributions of neutral keto- and enol-cytosine in the gas phase were calculated at the B3LYP/6-31G(d) level of theory by using natural population analysis (Figure 8). The results show that the addition sites preferred by radical **c** (based on transition state calculations), including N3 and carbonyl oxygen of the keto tautomer and N1 of the enol tautomer, are electron rich. This finding is in agreement with the electrophilic nature of the radicals studied. C5 position is calculated to be slightly more electron-rich than C6. Both C2 and C4 positions are highly electron deficient.

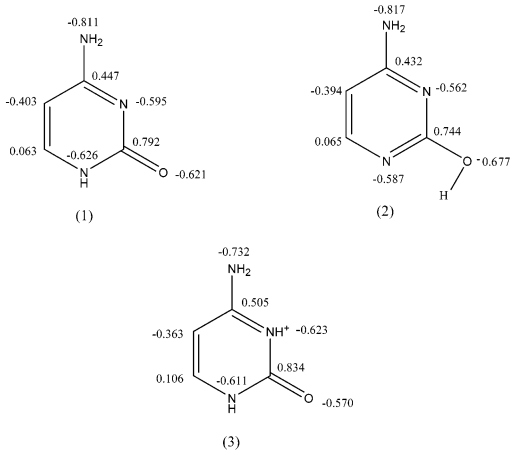

Figure 8. Charge distributions of cytosine based on natural population analysis. (1) Neutral keto-cytosine in the gas phase. (2) Neutral enol-cytosine in the gas phase. (3) N3-protonated keto cytosine in the acidic aqueous solution.

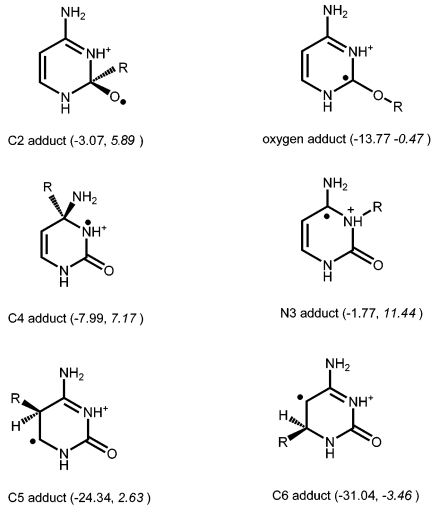

Figure 9. Structures of adducts possibly formed upon the reactions of N3-protonated keto-cytosine with the neutral phenyl radical (R) in acidic aqueous solution. The addition enthalpy changes and the energy barriers (in italics) are given in parentheses in kcal/mol.

In aqueous solution, the keto tautomer is the predominant tautomeric form of cytosine.[32] In acidic aqueous solution, the protonation of cytosine can occur and the preferred protonation site is N3.[32−34] The neutral 4-methoxyphenyl radical was found to attack C6 of cytosine under acidic conditions, while no adducts were found in neutral pH.[8] To theoretically explore the different addition site preferences, the enthalpy changes and the energy barriers for adduct formation between neutral phenyl radical (as a model of 4-methoxyphenyl radical) and N3-protonated keto-cytosine in aqueous solution were also estimated at the B3LYP/6-31G(d)+ZPVE level of theory using SCRF/Onsager model. The results are shown in Figure 9. The charge distribution of N3-protonated keto-cytosine in aqueous solution was also calculated using the SCRF/Onsager model (Figure 8). On the basis of these results, enthalpy changes and energy barriers predict the same addition site preferences in most cases.

(32) Colominas, C.; Luque, F. J.; Orozco, M. *J. Am. Chem. Soc.***1996**, *118*, 6811−6821.
(33) Florián, J.; Baumruk, V.; Leszczyński, J. *J. Phys. Chem.* **1996**, *100*, 5578−5589.
(34) Russo, N.; Toscano, M.; Grand, A.; Jolibois, F. *J. Comput. Chem.* **1998**, *19*, 989−1000.

Table 6. Overall Reaction Efficiencies and Product Branching Ratios[a] Measured for the Reactions of 1-Methylcytosine with Radicals **a**−**d**

		product branching ratios (%)					
radical	overall efficiency (%)	hydrogen abstraction	adduct	adduct-H	unknown ions *m/z* 187	adduct-pyridine	adduct-pyridine+H
a	40	11	34	0	55	0	0
b	27	64	17	0	0	13 *m/z* 201	6 *m/z* 202
c	18	81	13	0	0	4 *m/z* 201	2 *m/z* 202
d	3	11	77	0	0	7	5

[a] Overall efficiency and product branching ratios are the averaged values of several repeated experiments.

The addition of a neutral phenyl radical to the C6 position of N3-protonated keto-cytosine is the kinetically and thermodynamically most favored pathway, followed by C5, carbonyl oxygen (C5 is thermodynamically favored but oxygen is kinetically preferred), C2, and C4. Due to the protonation of N3, this site is the kinetically and thermodynamically least preferred site of addition. These computational results are in agreement with the results of the earlier EPR experiments.[8]

In acidic aqueous solution, protonation makes cytosine more susceptible to the attack by the slightly nucleophilic neutral phenyl radical. C2 and C4 are calculated to be electron deficient, but steric hindrance impedes the nucleophilic attack from phenyl radical. N3 and oxygen sites are electron rich, and the corresponding adducts are kinetically unfavored. C5 and C6 positions are electron deficient compared to N3 and oxygen and less sterically hindered than C2 and C4. Therefore, these sites are likely to be most susceptible to phenyl radical addition. C6 is the more electron deficient of these two sites. Furthermore, C6 is more electron deficient in acidic solution than in the gas phase, which may explain why the C6 adduct was observed in EPR experiments only under acidic conditions.[8]

2. Reactions between Charged Phenyl Radicals and 1-Methylcytosine. To gain further insight into the reactions of phenyl radicals toward nucleobases, the radicals **a**−**d** were allowed to react with 1-methylcytosine that can only exist as the keto tautomer. The radicals' reactivity order is the same as for cytosine, **a** > **b** > **c** > **d**, and the total reaction efficiencies are 40%, 27%, 18%, and 3%, respectively (Table 6). Compared with the situation of cytosine, radical **a** reacts with 1-methylcytosine slower while radicals **b**, **c**, and **d** react faster. As the radical reactivity decreases from radical **a** to **d**, the branching ratio of hydrogen abstraction increases from 34% to 70% for cytosine, as mentioned above. For the reactions of 1-methylcytosine with radicals **a**, **b**, and **c**, the branching ratio for hydrogen abstraction also increases when the radical reactivity decreases, ranging from 11% for **a** to 81% for **c**. However, for radical **d**, the branching ratio for hydrogen abstraction is just slightly greater than that of radical **a**.

Due to the absence of the enol tautomer, there are only four possible sites for hydrogen abstraction in 1-methylcytosine. The possible structures (and their symbols) of the hydrogen abstraction products are shown in Figure 10. Their relative stabilities are listed in Table 7. Structure **CH_3-H** is the most stable one (6.3 kcal/mol lower in energy than structure **NH_2-H**). The orbital occupied by the unpaired electron on the methylene carbon atom

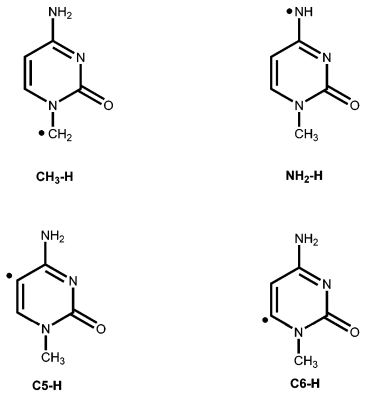

Figure 10. Structures of the products that may be formed upon hydrogen abstraction from 1-methylcytosine by radicals **a**−**d**.

Table 7. Relative Stabilities of the Different Hydrogen Abstraction Products That May Be Formed upon the Reactions between 1-Methylcytosine and Radicals **a**−**d** As Calculated at the B3LYP/6-31G(d)+ZPVE Level of Theory

product	electronic **E** (hartree)	ZPVE (hartree)	E + 0.9804ZPVE (hartree)	relative stability (kcal/mol)
CH_3−H	−433.5809496	0.1123050	−433.4708458	0.00
NH_2−H	−433.5713507	0.1127920	−433.4607694	6.32
C5−H	−433.5491024	0.1138010	−433.4375319	20.90
C6−H	−433.5565042	0.1131010	−433.4456200	15.83

Table 8. Enthalpy Changes[a] of Hydrogen Abstraction from 1-Methylcytosine by Radicals **a**−**d** As Calculated at the B3LYP/6-31G(d)+ZPVE Level of Theory (kcal/mol)

	product			
radical	**CH_3–H**	**NH_2–H**	**C5–H**	**C6–H**
a	−23.52	−17.20	−2.62	−7.70
b	−20.61	−14.28	0.30	−4.78
c	−20.51	−14.18	0.40	−4.68
d	−20.65	−14.33	0.25	−4.82

[a] Enthalpy changes were calculated directly from the enthalpies of reactants and products at 0 K.

in structure **CH_3-H** has π symmetry and is perpendicular to the cytosine ring. Hence, the unpaired electron of the CH_2 group can conjugate with the π electron system of the cytosine ring, which leads to the high stability of the structure. For structures **C5**−**H** and **C6**−**H**, the unpaired σ electron cannot interact with the π electron system of the cytosine ring, and hence these two structures are higher in energy. The enthalpy changes for hydrogen abstraction from all possible sites are shown in Table 8. These values were calculated directly because of a lack of a suitable reference systems for some of the necessary isodesmic reactions. For 1-methylcytosine, hydrogen abstraction from the methyl group is the most exothermic, followed by the amino group. Hydrogen abstraction from C5 is the least energetically favored.

Radicals **a**−**d** can form stable adducts with 1-methylcytosine. Only the adducts of radical **a** and 1-methylcytosine were theoretically investigated in this work. The six possible addition product structures are shown in Figure 11. All the structures were successfully optimized at the B3LYP/6-31G(d)+ZPVE level of theory except for the C2 adducts. Because of steric hindrance, the geometric optimization of C2 adducts failed to achieve convergence. It is reasonable to assume that the likelihood for the addition to C2 position is small. The directly calculated enthalpy changes for the formation of the other

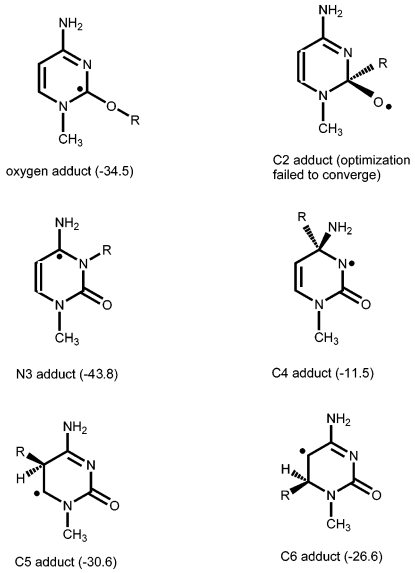

Figure 11. Structures of adducts possibly formed upon the gas-phase reactions of 1-methylcytosine with radical **a** (R). The calculated addition enthalpy changes are given in parentheses in kcal/mol.

adducts are also shown in Figure 11. The formation of all adducts is highly exothermic. The N3 adduct is the energetically most favored one (more stable than other adducts by at least 9.63 kcal/mol), followed by oxygen, C5, and C6 adducts. The C4 adduct is the energetically least preferred structure. The thermodynamically preferred addition sites in 1-methylcytosine for radicals **a**−**d** are similar to those of cytosine. On the basis of our calculations on reaction enthalpies and energy barriers for addition reactions of cytosine, kinetic factors (energy barriers) are likely to reflect the thermodynamic driving force also for 1-methylcytosine.

The adducts of 1-methylcytosine and radicals **b**−**d** can undergo dissociation by the loss of the neutral pyridine molecule. The dissociation products sometimes abstract a hydrogen atom from another 1-methylcytosine molecule to form closed shell cations as secondary products. In general, the branching ratios of this type of reaction products are not very high, ranging from 6% for radical **c** to 19% for radical **b**.

3. Unknown Products Formed upon the Reaction of Radical a with Cytosine. Comparison of the reactions of cytosine and 1-methylcytosine yields some information about the two unknown ions (*m*/*z* 172 and 173) formed upon the reaction of cytosine with radical **a**. For the reaction between 1-methylcytosine and radical **a**, there is only one unknown product ion (*m*/*z* 187) but with a relatively large branching ratio (55%). Therefore, one of the two unknown product ions observed in the case of cytosine might be related to the presence of the enol tautomer and therefore absent for 1-methylcytosine. Isotopically labeled 3-dehydro-*N*-(D_5-phenyl)pyridinium radical (generated by reaction of 3-iodopyridine with D_5-iodobenzene) reacts with cytosine and 1-methylcytosine to yield product ions with five units greater *m*/*z* values than for the unlabeled radical, *m*/*z* 177 and 178 for cytosine and *m*/*z* 192 for 1-methylcytosine. These results revealed that the benzene ring of the radical is conserved in the unknown product ions.

The fate of the cytosine ring in the reaction was examined using isotopically labeled 1,3,5-^{15}N-2,4-^{13}C-cytosine (the numbering scheme is illustrated in Figure 2). The branching ratios for radical **a** are 30% hydrogen abstraction product, 10% adduct, and 60% unknown product ion (*m*/*z* 177). Unlabeled cytosine reacts with radical **a** to yield 34% hydrogen abstraction product, 6% adduct, 2% adduct-H$^{\cdot}$, 28% unknown product ion of *m*/*z* 172, and 30% unknown product ion of *m*/*z* 173. Therefore, only one unknown product ion (*m*/*z* 177) was observed for labeled cytosine and its abundance was approximately the sum of the abundances of the two unknown ions (*m*/*z* 172 and 173) formed for unlabeled cytosine. It is concluded that the unknown product ion of *m*/*z* 173 contains only four of the five nitrogen and carbon atoms that were isotopically labeled in labeled cytosine, while the unknown product ion of *m*/*z* 172 contains all these five atoms. Therefore, both unknown product ions mentioned above have the same *m*/*z* of 177 for isotopically labeled cytosine.

Table 9. Overall Reaction Efficiencies and Product Branching Ratios Measured for the Reactions of Pyrimidine, 4-Aminopyrimidine, and 2-Hydroxypyrimidine with Radical **a**

		product branching ratios (%)				
					unknown ions	
neutral substrate	overall efficiency (%)	hydrogen abstraction	adduct	adduct-H	*m*/*z* 172	*m*/*z* 173
pyrimidine	8	4	68	28	0	0
4-aminopyrimidine	40	7	72	21	0	0
2-hydroxypyrimidine	1	36	51	0	0	13

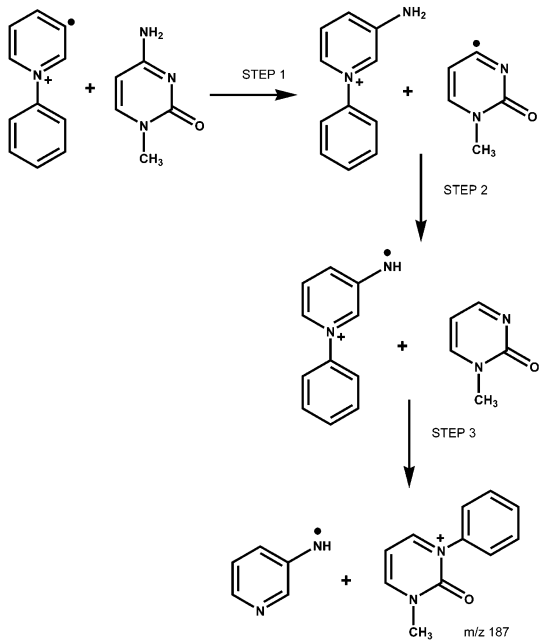

Figure 12. Possible mechanism for the formation of the ion of *m*/*z* 187 upon the reaction of 1-methylcytosine with radical **a**.

Examination of the reactions of 2-hydroxypyrimidine, 4-aminopyrimidine, and pyrimidine (Table 9) proves that the presence of a carbonyl group (keto form) or hydroxy group (enol form) is essential for the formation of the unknown product ions of *m*/*z* 172 and 173. Only 2-hydroxypyrimidine yields an unknown product ion of *m*/*z* 173. Since 2-hydroxypyrimidine does not have an amino group, it is reasonable to assume that the unknown product ion of *m*/*z* 172 formed upon the reaction of cytosine with radical **a** might contain the NH_2 group and the unknown product ion of *m*/*z* 173 might not. Figure 12 shows a possible mechanism for the formation of the unknown product ion of *m*/*z* 187 upon the reaction of 1-methylcytosine and radical **a** (corresponding to the formation of ion of *m*/*z* 173 for cytosine).

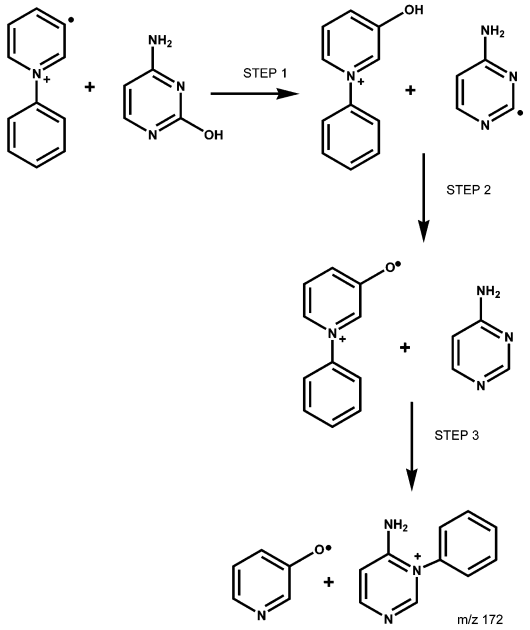

Figure 13. Possible mechanism for the formation of the ion of *m*/*z* 172 upon the reaction of cytosine with radical **a**.

The enthalpy changes of the first, second, and third steps of the reaction at 0 K were directly calculated at the B3LYP/6-31G(d)+ZPVE level of theory to be −9.0, −3.4, and −6.4 kcal/mol, respectively.

As mentioned above, the formation of the ion of *m*/*z* 172 for cytosine is likely related to the hydroxyl group of the enol tautomer. The possible structure and formation mechanism of the ion are shown in Figure 13. The directly calculated reaction enthalpy changes at the B3LYP/6-31G(d)+ZPVE level of theory are 0.8 kcal/mol for the first step, −12.7 kcal/mol for the second step, and 6.2 kcal/mol for the last step.

Conclusions

In contrast to aqueous solution where neutral phenyl radicals react with cytosine only by addition,[8] this study reveals that the positively charged phenyl radicals **a**−**d** react with cytosine in the gas phase by hydrogen abstraction and addition. Both reactions are accelerated upon increase in the radical's reactivity. The product branching ratios vary depending on the reactivity of the radicals: the less reactive the radical, the greater the branching ratio for the hydrogen abstraction products. These phenomena are consistent with the results of our previous investigations on thymine, uracil and adenine.[9] Transition state calculations for hydrogen abstraction from cytosine by charged phenyl radicals suggest that the reaction rate enhancement can be attributed to the lowering of the energy barrier. According to the ionic avoided curve crossing model,[26] this lowering is caused by the increasing electron deficiency at the radical site, which can be characterized by the vertical electron affinity of the radical. The favored site for hydrogen abstraction from cytosine by radicals **a**−**d**, based on computational evaluation of the energy barriers, enthalpy changes, and some relevant homolytic bond dissociation energies, is the amino group.

The theoretically predicted addition site for the radicals **a**−**d** in the gas phase is N3 for keto and N1 for enol cytosine. This result contradicts the previously reported addition site preference on C6 for neutral phenyl radicals in acidic aqueous phase (EPR experiments).[8] This discrepancy can be attributed to the electrophilic nature of radicals **a**−**d** and the nucleophilic nature of neutral phenyl radicals, and the different charge distribution of cytosine in the gas phase and acidic aqueous solution. The different addition site preference of cytosine in these different experiments implies that the mechanisms of DNA damage caused by radical attack may vary depending on the environmental conditions.

The reactions of 1-methylcytosine with radicals **a**−**d** also yield both addition and hydrogen abstraction products. For hydrogen abstraction, the energetically favored reaction site is calculated to be the methyl group while for addition reactions, N3 adducts are the most stable among all possible adduct structures.

The results presented here also suggest possible structures and formation mechanisms for two unknown product ions formed upon the reactions of cytosine with radical **a**. These ions are not formed for other nucleobases.[9]

Acknowledgment. This research project was partially supported by the National Institutes of Health.

JA021263R